Available online at www.sciencedirect.com
SCIENCE DIRECT
International Journal of Heat and Mass Transfer 49 (2006) 707–717
International Journal of HEAT and MASS TRANSFER
www.elsevier.com/locate/ijhmt

Nonlinear stability analysis of thin condensate falling film inside a rotating vertical cylinder

C.I. Chen [a,*], C.K. Chen [b], Y.T. Yang [b]

[a] Department of Industrial Engineering and Management, I-Shou University 1, Section 1, Hsueh-Cheng Road, Ta-Hsu Hsiang, Kaohsiung County, Taiwan 84041, Republic of China
[b] Department of Mechanical Engineering, National Cheng Kung University, Tainan, Taiwan 70101, Republic of China

Received 11 November 2004; received in revised form 17 August 2005
Available online 11 October 2005

Abstract

This paper investigates the stability of thin condensate film flowing down on the inner surface of a rotating vertical cylinder by means of long wave perturbation method in a two-step procedure. In the first step, the normal mode method is used to characterize the linear behavior. In the second step, an elaborated nonlinear film flow model is solved by using the method of multiple scales to characterize flow behavior at various states of sub-critical stability, sub-critical instability, supercritical stability, and supercritical explosion. The procedure follows the previous research [C.I. Chen, C.K. Chen, Y.T. Yang, Int. J. Heat Mass Transfer 47 (2004) 1937–1951] which concerns with the thin condensate falling film on the outer surface of a rotating vertical cylinder. The modeling results indicate that by increasing the rotation speed, Ω, and the radius of cylinder, R, the condensate film becomes more stable, which is totally opposite to the previous study.

Keywords: Thin film; Condensate; Rotation number; Ginzburg–Landau equation

1. Introduction

The stability problem of fluid film flowing down a vertical or inclined plate is commonly found in many engineering applications, such as heat exchangers, condensers, nuclear reactors. In practice, the condensate film flow easily forms waves, ripples or some other time-dependent phenomena. The waves, propagating at the film surface, increase the interfacial transfers. The further application to the stability analysis involves the coating of a moving solid substrate by a liquid layer.

The theory of laminar film condensation flow induced by gravity was first developed by Nusselt [2], but the stability problem of condensate falling flow had never been investigated until 1970s. Bankoff [3] used the long-wave perturbation method to study the linear instability problem of the film condensate flow. Without considering the temperature disturbance, the result showed that film condensation on a vertical wall is always unstable. Ünsal and Thomas [4] modified the kinematic condition by using the interfacial energy balance equation, and found the finite critical Reynolds number for the vertical wall. Essentially, the linear stability analysis can only be applied to study the cases of infinitesimal disturbances. When disturbance grows to be of a finite value, linear stability theory becomes invalid.

Extensive studies on the hydrodynamic stability problems regarding the condensate films flowing down a vertical wall or cylindrical surface have already been investigated by several researchers. Hung et al. [5] investigated the weakly nonlinear stability analysis of a condensate film flowing down the outer surface of vertical cylinder. They showed that supercritical stability in the linearly unstable region and sub-critical instability in the linearly stable region can co-exist. Du and Wang [6] studied the transport phenomena for flow film condensation in vertical

* Corresponding author. Tel.: +886 7 6577711x5522; fax: +886 7 6578536.
E-mail address: EddyChen@isu.edu.tw (C.I. Chen).

0017-9310/$ - see front matter © 2005 Elsevier Ltd. All rights reserved.
doi:10.1016/j.ijheatmasstransfer.2005.08.011

Nomenclature

C_p	specific heat of fluid
d	complex wave celerity $= d_r + \mathrm{i}d_i$
g	gravitational acceleration
h^*	film thickness
h_0^*	local base flow film thickness
h_{fg}	latent heat
K	thermal conductivity of the fluid
Nd	dimensionless parameter $= (1-\beta)\xi^2/\beta Pr^2$
p^*	fluid pressure
p_{g}^*	vapor pressure
Pe	local Peclect number $= PrRe$
Pr	Prandtl number $= \rho\nu C_p/K$
R^*	radius of cylinder
Re	Reynolds number $= u_0^* h_0^*/\nu$
Ro	Rotation number $= \Omega^* h_0^*/u_0^*$
r^*, z^*	coordinates transverse to and along the cylinder surface
S^*	surface tension of the fluid
t^*	time
T^*	fluid temperature
T_{s}^*	vapor saturation temperature
T_{w}^*	wall temperature
u_0^*	reference velocity $= gh_0^{*2}/4\nu\Gamma$
u^*, v^*, w^*	velocities along r^*-, θ^*- and z^*-directions, respectively

Greek symbols

α	dimensionless wave number
β	density ratio $= \rho_{\mathrm{g}}/\rho$
ε	infinitesimal parameter
ξ	Jakob number $= C_p(T_{\mathrm{s}}^* - T_{\mathrm{w}}^*)/h_{\mathrm{fg}}$
η	dimensionless perturbed film thickness
θ	dimensionless temperature
λ	perturbed wave length
μ	fluid dynamic viscosity
ν	fluid kinematic viscosity
ρ	fluid density
ρ_{g}	vapor density
Ω^*	constant angular velocity
φ	stream function

Superscripts

*	dimensional quantities
$'$	differentiation with respect to h

Subscripts

t, r, z	partial differentiation with respect to the subscript
0, 1, 2,...	expansion order of the long wave

mini-tube. Miyara et al. [7] investigated the condensation heat transfer and flow pattern inside a herringbone-type micro-fin tube. Furthermore, Miyara [8] studied the wave evolution and heat transfer behavior of a wavy condensate film down a vertical wall by a finite difference. The results showed that a circulation flow occurs in the large wave and it affects the temperature field. The heat transfer is enhanced by space-time film thickness variation and convection effects. Usha and Uma [9] considered the weakly nonlinear problem of condensate/evaporating power-law liquid film down an inclined plane. They [10] further conducted the research about interfacial phase change effects on the stability characteristics of thin viscoelastic liquid film down a vertical wall.

Condensate films developed on the vertical cylinders have received a reasonable amount of attention in the literatures, but how condensate films affected by the rotation have not been fully explored. The authors previously studied the thin condensate film falling on the outer surface of a rotating vertical cylinder [1]. In this paper, the falling condensate film inside the rotating vertical is reexamined to show the difference between these two cases.

2. Mathematical modeling

In this study, the axisymmetric flow of an incompressible, condensate liquid on the inner surface of a vertical cylinder which rotates with a constant velocity Ω^* is considered. The asterisk represents that this physical parameter is a dimensional quantity. The appropriate physical configuration is shown schematically in Fig. 1. In this case, all associated physical properties and the rate of film flow are assumed to be constant (i.e. time-invariant). Cylindrical polar coordinates (r^*, θ^*, z^*) are used, where r^* denotes the radial direction, θ^* denotes the circumferential direction, and z^* denotes the axial direction. The liquid-air interface is located at $r^* = R^* - h^*(z^*,t^*)$, where R^* is the cylinder radius and h^* is the film thickness. The equations of motion and continuity for axisymmetric flow can be expressed as

$$\frac{1}{r^*}\frac{\partial(r^*u^*)}{\partial r^*} + \frac{\partial w^*}{\partial z^*} = 0, \tag{1}$$

$$\frac{\partial u^*}{\partial t^*} + u^*\frac{\partial u^*}{\partial r^*} + w^*\frac{\partial u^*}{\partial z^*} - \frac{v^{*^2}}{r^*} = -\frac{1}{\rho}\frac{\partial p^*}{\partial r^*} + \frac{\mu}{\rho}\left(\frac{1}{r^*}\frac{\partial}{\partial r^*}\left(r^*\frac{\partial u^*}{\partial r^*}\right) - \frac{u^*}{r^{*^2}} + \frac{\partial^2 u^*}{\partial z^{*2}}\right), \tag{2}$$

$$\frac{\partial w^*}{\partial t^*} + u^*\frac{\partial w^*}{\partial r^*} + w^*\frac{\partial w^*}{\partial z^*} = -\frac{1}{\rho}\frac{\partial p^*}{\partial z^*} + g + \frac{\mu}{\rho}\left(\frac{1}{r^*}\frac{\partial}{\partial r^*}\left(r^*\frac{\partial w^*}{\partial r^*}\right) + \frac{\partial^2 w^*}{\partial z^{*2}}\right), \tag{3}$$

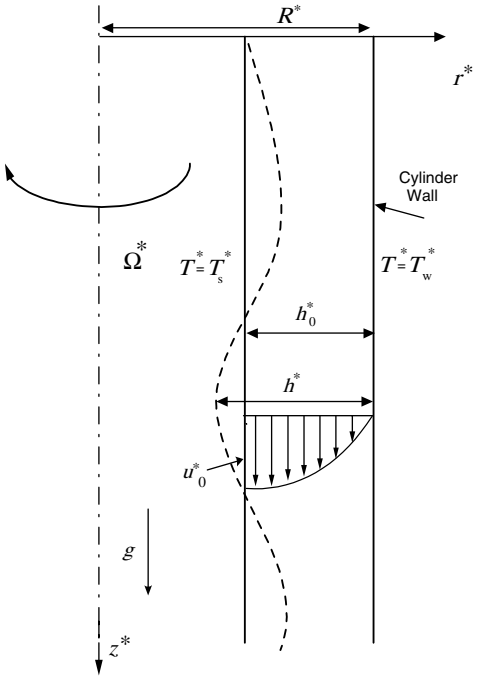

Fig. 1. Schematic diagram of a thin condensate film flow traveling down along the inner surface of a rotating vertical cylinder.

$$\frac{\partial T^*}{\partial t^*}+u^*\frac{\partial T^*}{\partial r^*}+w^*\frac{\partial T^*}{\partial z^*}=\frac{K}{\rho C_p}\left(\frac{1}{r^*}\frac{\partial}{\partial r^*}\left(r^*\frac{\partial T^*}{\partial r^*}\right)+\frac{\partial^2 T^*}{\partial z^{*2}}\right), \tag{4}$$

where T^*, ρ, p^*, μ, C_p and K are the fluid temperature, density, pressure, dynamic viscosity, specific heat and the thermal conductivity of the fluid, respectively.

For simplification, it is assumed that the fluid film flowing down the cylinder surface is very thin. In view of this, it is reasonable to assume that the tangential velocity is a constant throughout the radial direction in the thin film, i.e. $v^*=R^*\Omega^*$.

The boundary conditions on the inner wall of the cylinder at $r^*=R^*$ are given as

$$u^*=0,\quad w^*=0,\quad T^*=T^*_{\mathrm{w}}. \tag{5}$$

The boundary conditions at the free surface $r^*=R^*-h^*$ are based on the results given by Edwards et al. [11].

$$2\left(\frac{\partial u^*}{\partial r^*}-\frac{\partial w^*}{\partial z^*}\right)\frac{\partial h^*}{\partial z^*}-\left(\frac{\partial u^*}{\partial z^*}+\frac{\partial w^*}{\partial r^*}\right)\left[1-\left(\frac{\partial h^*}{\partial z^*}\right)^2\right]=0, \tag{6}$$

$$p^*+\frac{k^2(\beta-1)}{h_{\mathrm{fg}}^2\rho\beta}\left(\frac{\partial T^*}{\partial r^*}-\frac{\partial h^*}{\partial z^*}\frac{\partial T^*}{\partial z^*}\right)^2\left[1+\left(\frac{\partial h^*}{\partial z^*}\right)^2\right]^{-1}-2\rho\nu\left[\frac{\partial u^*}{\partial r^*}+\left(\frac{\partial w^*}{\partial r^*}+\frac{\partial u^*}{\partial z^*}\right)\frac{\partial h^*}{\partial z^*}+\frac{\partial w^*}{\partial z^*}\left(\frac{\partial h^*}{\partial z^*}\right)^2\right]$$
$$\times\left[1+\left(\frac{\partial h^*}{\partial z^*}\right)^2\right]^{-1}+S^*\left\{\frac{\partial^2 h^*}{\partial z^{*2}}\left[1+\left(\frac{\partial h^*}{\partial z^*}\right)^2\right]^{-3/2}+\frac{1}{r}\left[1+\left(\frac{\partial h^*}{\partial z^*}\right)^2\right]^{-1/2}\right\}=p^*_{\mathrm{g}}, \tag{7}$$

$$T^*=T^*_{\mathrm{s}}. \tag{8}$$

The kinematic condition that the flow cannot travel across a free surface can be described as

$$K\left(\frac{\partial T^*}{\partial r^*}-\frac{\partial T^*}{\partial z^*}\frac{\partial h^*}{\partial z^*}\right)-\rho h_{\mathrm{fg}}\left(u^*+w\frac{\partial h^*}{\partial z^*}+\frac{\partial h^*}{\partial t^*}\right)=0, \tag{9}$$

where T^*_{s} is vapor saturation temperature, T^*_{w} is wall temperature, p^*_{g} is the vapor pressure, S^* is the surface tension and h_{fg} is the latent heat of phase change.

By introducing the stream function, φ^*, into dimensional velocity components, the governing equation and boundary condition become

$$u^*=\frac{1}{r^*}\frac{\partial\varphi^*}{\partial z^*},\quad w^*=-\frac{1}{r^*}\frac{\partial\varphi^*}{\partial r^*}. \tag{10}$$

It is customarily to define flow associated dimensionless quantities as

$$z=\frac{\alpha z^*}{h_0^*},\quad r=\frac{r^*}{h_0^*},\quad R=\frac{R^*}{h_0^*},\quad t=\frac{\alpha u_0^* t^*}{h_0^*},\quad h=\frac{h^*}{h_0^*},$$
$$\varphi=\frac{\varphi^*}{u_0^* h_0^{*2}},\quad p=\frac{p^*-p^*_{\mathrm{g}}}{\rho u_0^{*2}},\quad Re=\frac{u_0^* h_0^*}{\nu},$$
$$S=\left(\frac{S^{*3}}{2^4\rho^3\nu^4 g}\right)^{1/3},\quad \alpha=\frac{2\pi h_0^*}{\lambda},\quad \theta=\frac{T^*-T^*_{\mathrm{w}}}{T^*_{\mathrm{s}}-T^*_{\mathrm{w}}},$$
$$Pr=\frac{\rho\nu C_{\mathrm{p}}}{K},\quad Pe=PrRe,\quad Nd=\frac{(1-\beta)\xi^2}{\beta Pr^2}, \tag{11}$$

where h_0^* is the constant film thickness of local base flow, u_0^* is the reference velocity, g is the gravitational acceleration, Pr is the Prandtl number, Pe is the Peclect number, Re is the Reynolds number, R is the dimensionless radius of the cylinder, φ is dimensionless stream function, α is the dimensionless wave number, ξ is the Jokob number, β is density ratio, S is dimensionless surface tension and λ is the wavelength.

In order to investigate the effect of angular velocity, Ω^*, on the stability of the flow field, the dimensionless Rotation number, is introduced

$$Ro=\frac{\Omega^* h_0^*}{u_0^*}. \tag{12}$$

u_0^* can be expressed as

$$u_0^*=\frac{g h_0^{*2}}{4\nu\Gamma}, \tag{13}$$

where $\Gamma=[2(R-1)^2\ln(\frac{R-1}{R})+(2R-1)]^{-1}$.

Assuming that $\alpha\ll 1$, the non-dimensional governing equations and the associated boundary conditions can be expressed as

$$p_r = \alpha[Re^{-1}(r^{-1}\varphi_{rrz} - r^{-2}\varphi_{rz})] + Ro^2\frac{R^2}{r} + \mathrm{O}(\alpha^2), \tag{14}$$

$$r^{-1}(r(r^{-1}\varphi_r)_r)_r = 4\Gamma + \alpha Re(-p_z + r^{-1}\varphi_{tr} + r^{-2}\varphi_z\varphi_{rr} - r^{-3}\varphi_z\varphi_r - r^{-2}\varphi_r\varphi_{rz}) + \mathrm{O}(\alpha^2), \tag{15}$$

$$r^{-1}(r\theta_r)_r = \alpha Pe(\theta_t - r^{-1}\varphi_r\theta_z + r^{-1}\varphi_z\theta_r) + \mathrm{O}(\alpha^2). \tag{16}$$

At the cylinder surface ($r = R$)

$$\varphi_r = \varphi_z = \theta = 0. \tag{17}$$

At free surface ($r = R - h$)

$$(r^{-1}\varphi_r)_r = \mathrm{O}(\alpha^2), \tag{18}$$

$$p = -2S\cdot Re^{-5/3}(2\Gamma)^{1/3}(\alpha^2 h_{zz} + r^{-1}) + \alpha\{-2Re^{-1}[(r^{-2}\varphi_r - r^{-1}\varphi_{rr})h_z + r^{-2}\varphi_z - r^{-1}\varphi_{rz}]\} - Nd\cdot Re^{-2}\cdot\theta_r^2 + \mathrm{O}(\alpha^2), \tag{19}$$

$$\theta = 1, \tag{20}$$

$$\xi\cdot(\theta_r - \alpha^2\theta_z h_z) - \alpha Pe(r^{-1}\varphi_z - r^{-1}\varphi_r h_z + h_t) = 0, \tag{21}$$

where the subscripts r, z, rr, zz and rz are used to represent various partial derivatives of the associated underlying variables.

Since the modes of long-wavelength that gives the smallest wave number are most likely to induce flow instability for the film flow [12,13], the dimensionless wave number of the long-wavelength mode, α, can then be chosen as the perturbation parameter for variable expansion. The stream function and flow pressure can be perturbed and represented as

$$\varphi = \varphi_0 + \alpha\varphi_1 + \mathrm{O}(\alpha^2), \quad p = p_0 + \alpha p_1 + \mathrm{O}(\alpha^2), \quad \theta = \theta_0 + \alpha\theta_1 + \mathrm{O}(\alpha^2). \tag{22}$$

The flow conditions of the thin film can be obtained by inserting the above expressions into Eqs. (14)–(20) and then solving systematically the resulting equations. In practical application, the non-dimensional surface tension S is a large value and the term $\alpha^2 S$ is taken to be of order one [9,10,14,15]. Further, in the analysis, $Re \simeq \mathrm{O}(1)$ and $Pe \simeq \mathrm{O}(1)$. By collecting all terms of zeroth order α^0 in the governing equations and boundary conditions, the solutions of zeroth order equations can now be expressed as

$$\varphi_0 = \Gamma\left[\frac{1}{4}(r^4 + R^4) - \frac{1}{2}R^2r^2 + \frac{1}{2}q^2(r^2 - R^2) - q^2r^2\ln\frac{r}{R}\right], \tag{23}$$

$$\theta_0 = \left(\ln\frac{r}{R}\right)\cdot(\ln Q)^{-1}, \tag{24}$$

$$p_0 = -2S\cdot Re^{-5/3}(2\Gamma)^{1/3}\left(\alpha^2 h_{zz} + \frac{1}{q}\right) + Ro^2R^2\ln\frac{r}{q} - Nd\cdot(Re\cdot\ln Q\cdot q)^{-2}, \tag{25}$$

where $q = R - h$, $Q = q/R$.

Similarly, after collecting all terms of first order α^1 in the governing equations and boundary conditions, the solutions of first order equations can now be obtained and expressed in the Appendix A.

The zeroth and the first order solutions are inserted into the dimensionless free surface kinematic equation (21) to yield the following generalized nonlinear kinematic equation

$$h_t + X(h) + A(h)h_z + B(h)h_{zz} + C(h)h_{zzzz} + D(h)h_z^2 + E(h)h_z h_{zzz} = 0, \tag{26}$$

where $X(h)$, $A(h)$, $B(h)$, $C(h)$, $D(h)$ and $E(h)$ are given in Appendix B.

3. Stability analysis

As the variation of the film thickness of the base flow is found to be very small for $|\alpha h_x| \ll 1$ using an analysis based on Nusselt assumption, the dimensionless film thickness when expressed in perturbed state can be given as

$$h(t,z) = 1 + \eta(t,z), \tag{27}$$

where $\eta(t,z)$ is a perturbed quantity to the stationary film thickness. The approximation $|\alpha h_x| \ll 1$ give the qualitative results for the constant film thickness assumption at the zero order. It is important to note that this constant film thickness approximations with long wave perturbations are reasonable approximations only for certain segments of weakly condensing flow. As has been pointed out by Joo et al. [16] and Burelbach et al. [17], the condensate films do not allow a steady uniform basic state. If the basic state is uniform, it must be time-dependent. However, the analysis in this study is based on the locally valid unsteady equation under the assumption of steady state undisturbed liquid film which can simplify the analysis and computations. By inserting the Eq. (27) into Eq. (26) and collecting all terms up to the order of η^3, the evolution equation of η becomes

$$\eta_t + X'\eta + A\eta_z + B\eta_{zz} + C\eta_{zzzz} = -\left[\frac{X''}{2}\eta^2 + \frac{X'''}{6}\eta^3 + \left(A'\eta + \frac{A''}{2}\eta^2\right)\eta_z + \left(B'\eta + \frac{B''}{2}\eta^2\right)\eta_{zz} + \left(C'\eta + \frac{C''}{2}\eta^2\right)\eta_{zzzz} + (D + D'\eta)\eta_z^2 + (E + E'\eta)\eta_z\eta_{zzz}\right] + \mathrm{O}(\eta^4). \tag{28}$$

The values of X, A, B, C, D, and E and their derivatives are all evaluated at the dimensionless height, $h = 1$, of the film flow.

3.1. Linear stability analysis

As the nonlinear terms in Eq. (28) are neglected, the linearized equation is obtained as

$$\eta_t + X'\eta + A\eta_z + B\eta_{zz} + C\eta_{zzzz} = 0. \tag{29}$$

The normal mode analysis method can be performed by assuming that

$$\eta = a\exp[\mathrm{i}(z - \mathrm{d}t)] + \text{c.c.}, \tag{30}$$

where a is the perturbation amplitude, and c.c. is the complex conjugate counterpart. The complex wave celerity, d, is given as

$$d = d_r + \mathrm{i}d_i = A + \mathrm{i}(B - C - X'), \tag{31}$$

where d_r is the linear wave speed, and d_i is the linear growth rate of the wave amplitudes. The flow is in linearly unstable supercritical condition if $d_i > 0$, and is in linearly stable sub-critical condition if $d_i < 0$.

3.2. Nonlinear stability analysis

By the method of multiple scales [18], the Ginzburg–Landau equation [19] can be derived following the same procedure as Chen et al. [1]

$$\frac{\partial a}{\partial t_2} + D_1 \frac{\partial^2 a}{\partial z_1^2} - \varepsilon^{-2} d_i a + (E_1 + \mathrm{i}F_1)a^2 \bar{a} = 0, \tag{32}$$

where

$$e = e_r + \mathrm{i}e_i = \frac{-\left(\frac{X''}{2} - B' + C' - D + E\right)}{16C - 4B + X} + \mathrm{i}\frac{-A'}{16C - 4B + X}, \tag{33}$$

$$D_1 = B - 6C, \tag{34}$$

$$E_1 = (X'' - 5B' + 17C' + 4D - 10E)e_r - A'e_i + \left(\frac{1}{2}X''' - \frac{3}{2}B' + \frac{3}{2}C'' + D' - E'\right), \tag{35}$$

$$F_1 = (X'' - 5B' + 17C' + 4D - 10E)e_i + A'e_r + \frac{1}{2}A''. \tag{36}$$

The overhead bar appearing in equation (32) stands for the complex conjugate of the same variable. In order for a supercritical stable region to exist in the linearly unstable region ($d_i > 0$), the condition is given as $E_1 > 0$. The associated wave amplitude εa_0 in the supercritical stable region is obtained as

$$\varepsilon a_0 = \sqrt{\frac{d_i}{E_1}}. \tag{37}$$

The nonlinear wave speed is given by

$$Nc_r = d_r + d_i\left(\frac{F_1}{E_1}\right). \tag{38}$$

The Ginzburg–Landau equation can be used to characterize various flow states and the results are customarily summarized and presented as Landau table [20].

4. Results and discussion

In order to study the influence of rotation and the radius of cylinder on the stability of the film flow, physical parameters selected for this study include (1) Reynolds number Re: 0–15, (2) wave numbers α: 0–0.12, (3) Rotation number Ro: 0, 0.1, 0.2 and (4) cylinder radius R: 10, 20, 50, 100. For the purpose of comparison with the literature [5,21], the values of dimensional quantities are taken as, a constant dimensionless surface tension $S = 6173.5$ [14,15], Jokob number, $\xi = 0.0872$; Prandtl number, $Pr = 2.62$, density ratio, $\beta = 0.000611$, and $Nd = 1.812$. The temperature at the interface is taken as $T_s^* = 373$ K and the temperature difference between the wall and the interface as $\Delta T^* = T_s^* - T_w^* = 47$ K. The above physical quantities are taken from the condensate water at the temperature of $T_w^* + \Delta T/3$ except for surface tension at 373 K. The pressure condition is at 1 atm.

4.1. Linear stability analysis

By setting $d_i = 0$ in the linear stability analysis, the neutral stability curve can be easily determined from Eq. (31). The α–Re plane is divided into two different characteristic regions by the neutral stability curve. One is the linearly stable region where small disturbances decay with time and the other is the linearly unstable region where small perturbations grow as time increases. Fig. 2(a) shows the neutral stability curves of a condensate film falling with

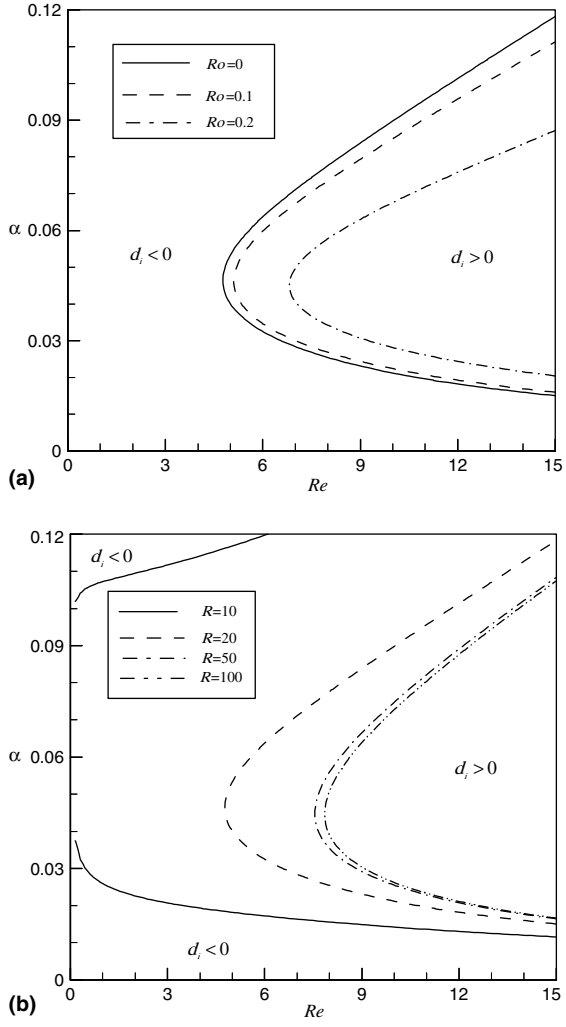

Fig. 2. Neutral stability curves for various (a) Ro values at $R = 20$; (b) R values at $Ro = 0$.

various values of Rotation number. The results indicate that the area of linearly stable region ($d_i < 0$) enlarges as the rotating speed increases. Fig. 2(b) shows the neutral stability curves of a stationary ($Ro = 0$) vertical cylinder with different values radii. The results indicate that the area of linearly unstable region ($d_i > 0$) becomes larger for a decreasing R. Namely; a cylinder with smaller radius induces the flow instability condition. The results indicate that the area of linearly stable region ($d_i < 0$) enlarges significantly by the existence of rotation motion. The temporal growth rate of the film flow is also computed by using Eq. (31). Fig. 3(a) and (b) shows the temporal film growth rate of a condensate film at $Ro = 0.1$, 0.2 and $Ro = 0$. It is interesting to note that temporal film growth rate decreases as the value of Ro increases and Re decreases. Furthermore, it is found that both the wave number of neutral mode and the maximum temporal film growth rate decrease as the value of Ro increases. Fig. 3(c) and (d) show the temporal film growth rate in rotating case of which Rotation number is equal to 0.1 at $R = 10$, 20, 50 and 100. It is noted that temporal film growth rate decreases as the value of R increases. That is, the larger the value of radius R is, the higher the stability of a liquid film.

4.2. Nonlinear stability analysis

As the perturbed wave grows to finite amplitude, the linear stability theory is no longer valid for accurate prediction of flow behavior. The nonlinear stability analysis is used here to study the effect of finite amplitude disturbances on the change of stability behaviors in the linearly stable region. For example, by using the same nonlinear flow stability, one can characterize the flow behaviors that subsequent nonlinear evolution of disturbances in the linearly unstable region may be redeveloped to a new equilibrium state of finite amplitudes (i.e. supercritical stability) or become unstable. If E_1 in Eq. (35) is a negative value, the amplitude of disturbed waves in the linearly stable region is possible to develop to a unstable state, even though the prediction obtained by linear analysis always gives stable

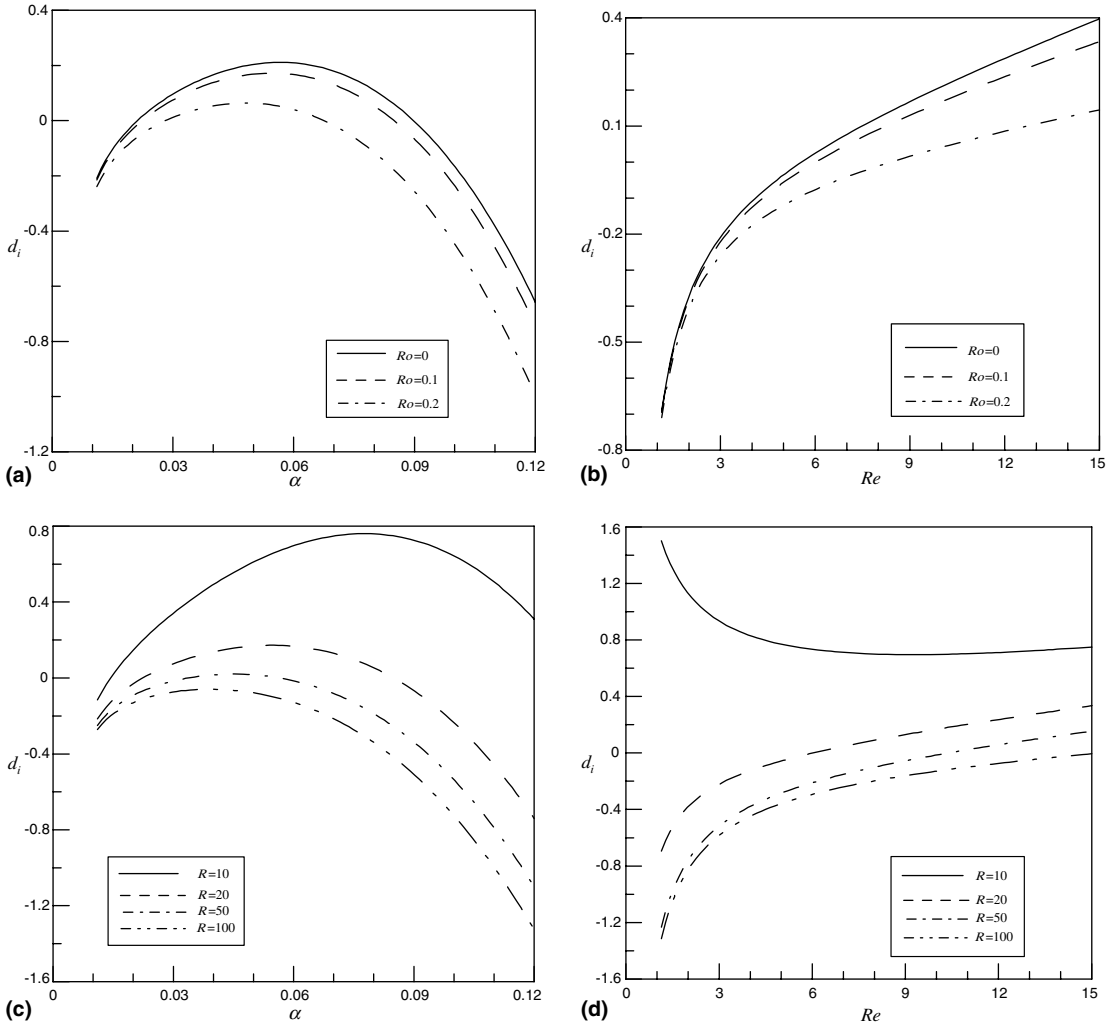

Fig. 3. Amplitude growth rate of disturbed waves in condensate flows for various (a) Ro values at $Re = 10$, $R = 20$; (b) Ro values at $\alpha = 0.06$, $R = 20$; (c) R values at $Re = 10$, $Ro = 0.1$; (d) R values at $\alpha = 0.06$, $Ro = 0.1$.

result. The nonlinear neutral stability curves can be obtained by simultaneously setting both $d_i = 0$ for Eq. (31) and $E_1 = 0$ for Eq. (35). The hatched areas in Fig. 4(a)–(d) reveals that various conditions for the sub-critical instability ($d_i < 0, E_1 < 0$), the sub-critical stability ($d_i < 0$, $E_1 > 0$), the supercritical stability ($d_i > 0, E_1 > 0$), and the explosive supercritical instability ($d_i > 0, E_1 < 0$) are possibly to occur for different rotating speed.

Fig. 4(a)–(c) show that the neutral stability curves of $d_i = 0$ and $E_1 = 0$ are shifted downward as the value of Ro increases. Therefore, the area of shaded sub-critical instability region ($d_i < 0, E_1 < 0$) increases and the area of shaded supercritical instability region ($d_i > 0, E_1 < 0$) decreases as the value of Ro increases. The area of supercritical stability region ($d_i > 0, E_1 > 0$) decreases and the area of sub-critical stability region ($d_i < 0, E_1 > 0$) increase as the values of Ro increase. Fig. 4(b) and (d) show that the neutral stability curves of $d_i = 0$ and $E_1 = 0$ are shifted upward as the value of R decreases. Therefore, the area of shaded sub-critical instability region increases and the area of shaded supercritical instability region decreases as the value of R increases. The area of supercritical stability region increases and the area of sub-critical stability region decrease as the value of R decreases.

Fig. 5(a) shows the threshold amplitude in sub-critical unstable region for various wave numbers with different Ro values at $Re = 10$ and $R = 20$. The results indicate that the threshold amplitude εa_0 becomes larger as the value of rotating parameter Ro increases. Fig. 5(b) shows the threshold amplitude in sub-critical unstable region for various wave numbers with different values of radius R at $Re = 10$ and $Ro = 0.1$. The results indicate that the threshold amplitude εa_0 becomes smaller as the value of radius R decreases. In such situations, the condensate film which holds the higher threshold amplitude value becomes more stable than that holds smaller one.

In the linearly unstable region, the linear amplification rate is positive, while the nonlinear amplification rate is negative. Therefore, a linear infinitesimal disturbance in the unstable region, instead of becoming infinite, will reach

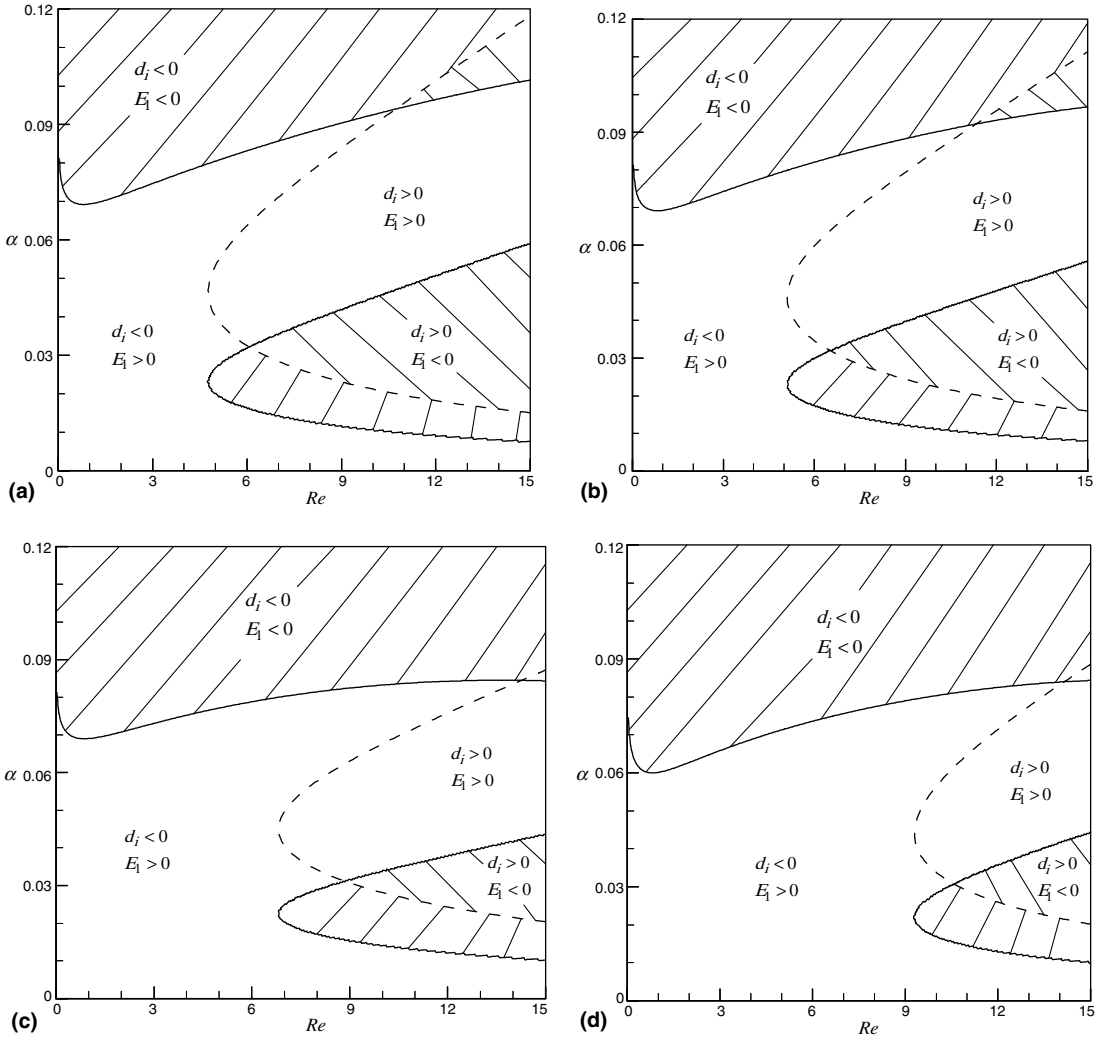

Fig. 4. Neutral stability curve of condensate film flows for (a) $Ro = 0$, $R = 20$; (b) $Ro = 0.1$, $R = 20$; (c) $Ro = 0.2$, $R = 20$; (d) $Ro = 0.1$, $R = 50$.

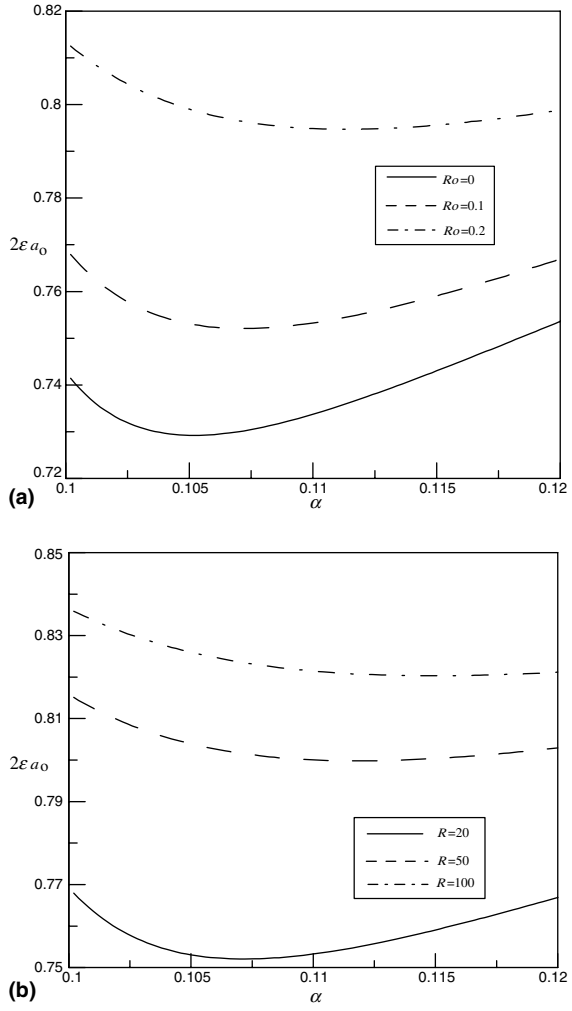

Fig. 5. Threshold amplitude in sub-critical unstable region for three different (a) R values at $Re = 10$, $Ro = 0.1$; (b) Ro values at $Re = 10$, $R = 20$.

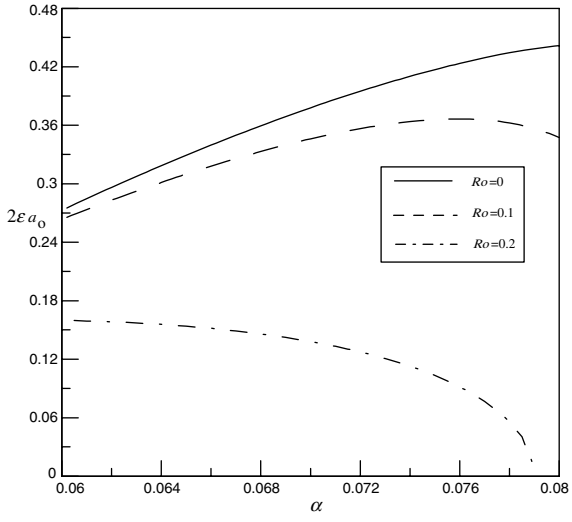

Fig. 6. Threshold amplitude in supercritical stable region for three different Ro values at $Re = 10$, $R = 20$.

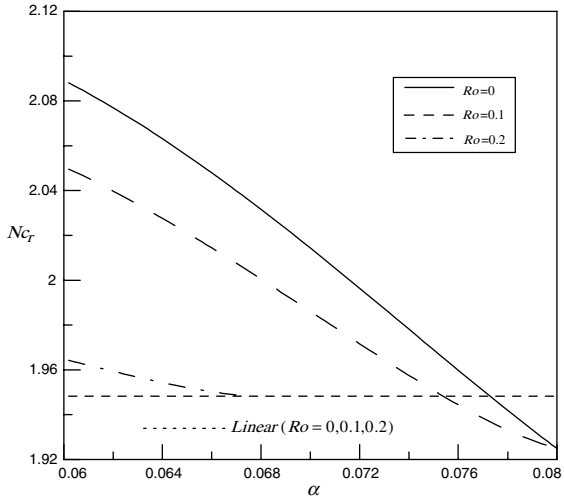

Fig. 7. Nonlinear wave speed in supercritical stable region for three different Ro values at $Re = 10$, $R = 20$.

finite equilibrium amplitude as given in Eq. (32). Fig. 6 shows the threshold amplitude in the supercritical stable region for various wave numbers under different values of rotating parameter Ro at $Re = 10$ and $R = 20$. It is found that the increase of Ro will lower the threshold amplitude, and the flow become comparatively stable.

The wave speed of Eq. (31) predicted by the linear theory is a constant value for all wave number and rotating parameter Ro. However, the wave speed of Eq. (38) predicted by using nonlinear theory is no longer a constant. It is actually a function of wave number, Reynolds number, Rotation number, and the radius of cylinder. Fig. 7 shows the nonlinear wave speed in the supercritical region for various perturbed wave numbers and different Rotation numbers $Ro = 0$, 0.1, 0.2 at $Re = 10$ and $R = 20$. It is found that the nonlinear wave speed increases as the value of Ro decreases.

5. Conclusions

The stability of a thin condensate film flowing down the inner surface of a rotating vertical cylinder is thoroughly investigated by using the method of long wave perturbation. The generalized nonlinear kinematic equation of the film flow at the interface of free surface is derived and numerically estimated to characterize the behaviors of flow stability under different Rotation number and radius of cylinder. Based on the results of numerical modeling, three conclusions can be made:

1. The results of linear stability analysis indicate that the area of linearly stable region becomes larger for an increasing Ro and R value. It is also noted that the temporal growth rate of film is reduced with a increasing Ro and R value. In other words, the degree of stability is enhanced if the flow is perturbed by waves with a higher rotation speed, and a greater radius of the cylinder.

2. In the nonlinear stability analysis, it is noted that the area of shaded sub-critical instability region and sub-critical stability region are increased as the value of *Ro* and *R* increase. On the other hand, the area of shaded supercritical instability region and supercritical stability region decrease with an increasing *Ro* and *R*. It is also shown that the threshold amplitude εa_0 in the sub-critical instability region increases as the value of *Ro* increases. Both the threshold amplitude and nonlinear wave speed in the supercritical stability region decrease with an increasing *Ro* value.
3. In this research, the rotation motion contributes the force which sticks the condensate film to the inner wall of a vertical rotating cylinder. On the contrary, if the condensate film is on the outer surface of a vertical rotating cylinder, the film will be detached from the surface due to the centrifugal force [1]. From these two researches, the rotation effect make the condensate film more stable when it is in the inner surface of cylinder, but the rotation effect make the film less stable when it is on the outer surface of cylinder.

Acknowledgements

The authors would like to thank the National Science Council of Republic of China for financially supporting this research under Contract No. NSC 93-2212-E-214-003. Also, the authors sincerely thank the referees for their very useful comments and suggestions which have helped in improving the quality of this manuscript.

Appendix A. First order solution

$$\varphi_1 = k_1 r^6 + k_2 r^4 + k_3 r^2 + k_4,$$

$$\theta_1 = b_1 r^4 + b_2 r^2 + b_3,$$

where

$$k_1 = -\frac{1}{48} Re\Gamma^2 q h_z,$$

$$\begin{aligned} k_2 = {} & \frac{1}{8} SRe^{-2/3}(2\Gamma)^{1/3}\left(\alpha^2 h_{zzz} + \frac{1}{q^2} h_z\right) \\ & - Re\Gamma q h_{0t}\left(\frac{5}{16} - \frac{1}{4}\ln\frac{r}{R}\right) \\ & - Re\Gamma^2 q h_z\left\{R^2\left(\frac{3}{16} - \frac{1}{4}\ln\frac{r}{R}\right)\right. \\ & \left. + q^2\left[-\frac{3}{2} + \frac{3}{2}\ln\frac{r}{R} - \frac{1}{2}\left(\ln\frac{r}{R}\right)^2\right]\right\} \\ & - ReRo^2\frac{R^2 h_z}{16q} + \frac{Nd(1+\ln Q)h_z}{8Re(q\ln Q)^3}, \end{aligned}$$

$$\begin{aligned} k_3 = {} & \frac{1}{4} SRe^{-2/3}(2\Gamma)^{1/3}\left(\alpha^2 h_{zzz} + \frac{1}{q^2} h_z\right)\left(q^2 - R^2 - 2q^2\ln\frac{r}{R}\right) \\ & - Re\Gamma h_{0t} q\left[q^2\left(\frac{1}{2}\ln Q - \frac{1}{4}\right)\left(2\ln\frac{r}{R} - 1\right) - \frac{1}{2}R^2\right] \\ & - Re\Gamma^2 q h_z\left\{-\frac{5}{16}R^4 + R^2 q^2\left[\frac{5}{2} - \frac{1}{2}\ln\frac{r}{R} + \frac{1}{2}\left(\ln\frac{r}{R}\right)^2\right]\right. \\ & + q^4\left[-\frac{7}{8} + \frac{3}{2}\ln Q + \frac{7}{4}\ln\frac{r}{R} - (\ln Q)^2 - 3\ln Q\cdot\ln\frac{r}{R}\right. \\ & \left.\left. + 2(\ln Q)^2\ln\frac{r}{R}\right]\right\} - ReRo^2\frac{R^2}{8q}\left(q^2 - R^2 - 2q^2\ln\frac{r}{R}\right)h_z \\ & + \frac{Nd(1+\ln Q)(q^2 - R^2 - 2q^2\ln\frac{r}{R})h_z}{4Re(q\ln Q)^3}, \end{aligned}$$

$$\begin{aligned} k_4 = {} & \frac{1}{8} SRe^{-2/3}(2\Gamma)^{1/3}\left(\alpha^2 h_{zzz} + \frac{1}{q^2} h_z\right)(R^4 - 2R^2 q^2) \\ & + Re\Gamma h_{0t} q\left[\frac{3}{16}R^4 + q^2 R^2\left(\frac{1}{2}\ln Q - \frac{1}{4}\right)\right] \\ & + Re\Gamma^2 q h_z\left\{\frac{5}{48}R^6 - R^4 q^2 + \frac{1}{8}R^2 q^4[7 - 12\ln Q + 8(\ln Q)^2]\right\} \\ & + ReRo^2\frac{R^4}{16q}(R^2 - 2q^2)h_z - \frac{NdR^2(R^2 - 2q^2)(1+\ln Q)h_z}{8Re(q\ln Q)^3}, \end{aligned}$$

$$b_1 = -\frac{1}{16} Pe\Gamma h_z q^{-1}(\ln Q)^{-2}\left(\ln\frac{r}{R} - \frac{1}{2}\right),$$

$$\begin{aligned} b_2 = {} & -\frac{1}{4} Peh_z q^{-1}(\ln Q)^{-2}\left(1 - \ln\frac{r}{R}\right) \\ & - Pe\Gamma h_z q^{-1}(\ln Q)^{-2}\left\{\frac{1}{4}R^2\left(1 - \ln\frac{r}{R}\right) - q^2\left[\frac{1}{2}\left(\ln\frac{r}{R}\right)^2\right.\right. \\ & \left.\left. - \ln\frac{r}{R} + \frac{3}{4}\right]\right\} - Pe\Gamma h_z q(\ln Q)^{-1}\left(\frac{3}{4} - \frac{1}{2}\ln\frac{r}{R}\right), \end{aligned}$$

$$\begin{aligned} b_3 = {} & -\frac{1}{4} Peh_{0t} q^{-1}(\ln Q)^{-3}\left[(R^2 + q^2\ln Q - q^2)\ln\frac{r}{R} - R^2\ln Q\right] \\ & - \frac{1}{2} PeqR^2\Gamma\ln\frac{r}{R}h_z \\ & - \Gamma Pe(\ln Q)^{-1}h_z\left[q^3\ln\frac{r}{R}\frac{3}{4}qR^2 - \frac{1}{2}qR^2\left(\ln\frac{r}{R}\right)^2\right] \\ & - \Gamma(\ln Q)^{-2}Peh_z\left[\left(qR^2 - \frac{29}{16}q^3\right)\ln\frac{r}{R} + \left(\frac{3}{4}qR^2 - \frac{7R^4}{32q}\right)\right] \\ & - Peh_z\Gamma\ln\frac{r}{R}(\ln Q)^{-3}\left(\frac{25}{32}q^3 - qR^2 + \frac{7R^4}{32q}\right), \end{aligned}$$

where $q = R - h$

$$Q = \frac{R-h}{R} = \frac{q}{R}$$

$$h_{0t} = 2\Gamma(q^2 - R^2 - 2q^2\ln Q)h_z + \frac{\xi}{\alpha Pe}(1 + \alpha^2 h_z^2)q^{-1}(\ln Q)^{-1}.$$

Appendix B. Generalized nonlinear kinematic equation

$$h_t + X(h) + A(h)h_z + B(h)h_{zz} + C(h)h_{zzzz} + D(h)h_z^2 + E(h)h_z h_{zzz} = 0,$$

where

$$X(h) = \frac{\varsigma}{\alpha Pe}[K_1(h) + \varsigma K_2(h)],$$

$$K_1(h) = q^{-1}(\ln Q)^{-1},$$

$$K_2(h) = \left[\frac{1}{4}q^{-3}(\ln Q)^{-4}(R^2 - q^2 + q^2\ln Q) - q^{-1}(\ln Q)^{-3}\left(\frac{1}{2}\ln Q - \frac{1}{4}\right)\right],$$

$$A(h) = K_3(h) + \varsigma K_4(h) + \frac{\varsigma}{Pr}K_5(h),$$

$$K_3(h) = 2\Gamma(R^2 - q^2 + 2q^2\ln Q),$$

$$K_4(h) = \Gamma\left\{\frac{1}{2}R^2 + \left(-\frac{1}{4}q^2 - \frac{1}{2}R^2\right)(\ln Q)^{-1} + \left(\frac{3}{8}q^2 + \frac{3}{4}R^2\right)(\ln Q)^{-2} + \frac{9}{32}\left(-q^2 + \frac{R^4}{q^2}\right)(\ln Q)^{-3}\right\},$$

$$K_5(h) = \Gamma\left\{(4q^2 - R^2) + \left(-\frac{9}{4}q^2 + \frac{3}{2}R^2\right)(\ln Q)^{-1} + \left(\frac{9}{16}q^2 - \frac{3}{4}R^2 + \frac{3R^4}{16q^2}\right)(\ln Q)^{-2} - 4q^2\ln Q\right\},$$

$$B(h) = \alpha SRe^{-2/3}(2\Gamma)^{1/3}K_6(h) + \alpha ReK_7(h) + ReRo^2\alpha K_8(h) + \frac{\alpha Nd}{Re}K_9(h),$$

$$K_6(h) = -\frac{1}{8}\left(4q\ln Q - 3q^3 + 4\frac{R^2}{q} - \frac{R^4}{q^3}\right),$$

$$K_7(h) = \Gamma^2\left\{\frac{13}{48}R^6 + \frac{1}{16}R^4q^2(-9 + 28\ln Q) + \frac{1}{48}q^6[59 - 120(\ln Q)^2 + 96(\ln Q)^3] + \frac{1}{16}R^2q^4[-15 - 8(\ln q)^2 - 68\ln Q + 16\ln q\cdot\ln Q + 32(\ln Q)^2 + 8(\ln R)^2]\right\},$$

$$K_8(h) = \frac{1}{16q^2}R^2(-3q^4 + 4q^2R^2 - R^4 + 4q^4\ln Q),$$

$$K_9(h) = \left\{\left(\frac{3}{8} - \frac{R^2}{2q^2} + \frac{R^4}{8q^4}\right)(\ln Q)^{-3} + \left(-\frac{1}{8} - \frac{R^2}{4q^2} + \frac{R^4}{8q^4}\right)(\ln Q)^{-2} - \frac{1}{2}(\ln Q)^{-1}\right\},$$

$$C(h) = -\frac{1}{8}\alpha^3 SRe^{-2/3}(2\Gamma)^{1/3}\left(4R^2q + 4q^3\ln Q - 3q^3 - \frac{R^4}{q}\right),$$

$$D(h) = \alpha SRe^{-2/3}(2\Gamma)^{1/3}K_{10}(h) + \alpha ReK_{11}(h) + ReRo^2\alpha K_{12}(h) + \frac{\alpha Nd}{Re}K_{13}(h) + \frac{\alpha\varsigma}{Pe}[K_{14}(h) + \varsigma K_{15}(h)],$$

$$K_{10}(h) = \frac{1}{4}\left(4\ln Q + \frac{R^4}{q^4} - 1\right),$$

$$K_{11}(h) = -\Gamma^2\left\{\frac{13R^6}{48q} + q^5\left[\frac{413}{48} - 5\ln Q - \frac{23}{2}(\ln Q)^2 + 14(\ln Q)^3\right] + R^4q\left(\frac{1}{16} + \frac{21}{4}\ln Q\right) + R^2q^3\left[-\frac{143}{16} - \frac{65}{4}\ln Q + \frac{25}{2}(\ln Q)^2\right]\right\},$$

$$K_{12}(h) = -\frac{1}{16q^3}R^2(-5q^4 + 4q^2R^2 + R^4 + 12q^4\ln Q),$$

$$K_{13}(h) = q^{-1}\left\{-\frac{1}{2}(\ln Q)^{-1} + \left(\frac{3}{8} + \frac{R^2}{2q^2} - \frac{3R^4}{8q^4}\right)(\ln Q)^{-2} + \left(\frac{5}{8} + \frac{3R^2}{2q^2} - \frac{5R^4}{8q^4}\right)(\ln Q)^{-3} + \left(-\frac{9}{8} + \frac{3R^2}{2q^2} - \frac{3R^4}{8q^4}\right)(\ln Q)^{-4}\right\},$$

$$K_{14}(h) = (q\ln Q)^{-1},$$

$$K_{15}(h) = -q^{-1}\left[(\ln Q)^{-2} - (\ln Q)^{-3} + \frac{1}{2}\left(1 - \frac{R^2}{q^2}\right)(\ln Q)^{-4}\right],$$

$$E(h) = \alpha^3 SRe^{-2/3}(2\Gamma)^{1/3}(R^2 - q^2 + 2q^2\ln Q).$$

References

[1] C.I. Chen, C.K. Chen, Y.T. Yang, Perturbation analysis to the nonlinear stability characterization of thin condensate falling film on the outer surface of a rotating vertical cylinder, Int. J. Heat Mass Transfer 47 (2004) 1937–1951.

[2] W. Nusselt, Die Oberflachenkondensation des Wasserdampfes, Z. VDI 50 (1916) 541–546.

[3] S.G. Bankoff, Stability of liquid flow down a heated inclined plane, Int. J. Heat Mass Transfer 14 (1971) 377–385.

[4] M. Ünsal, W.C. Thomas, Linearized stability analysis of film condensation, ASME J. Heat Transfer 100 (1978) 629–634.

[5] C.I. Hung, C.K. Chen, J.S. Tsai, Weakly nonlinear stability analysis of condensate film flow down a vertical cylinder, Int. J. Heat Mass Transfer 39 (1996) 2821–2829.

[6] X.E. Du, B.X. Wang, Study on transport phenomena for flow film condensation in vertical mini-tube with interfacial waves, Int. J. Heat Mass Transfer 46 (2003) 2095–2101.

[7] A. Miyara, K. Nonaka, M. Taniguchi, Condensation heat transfer and flow pattern inside a herringbone-type micro-fin tube, Int. J. Refrigeration 23 (2000) 141–152.

[8] A. Miyara, Flow dynamics and heat transfer of wavy condensate film, ASME J. Heat Transfer 123 (2001) 492–500.

[9] R. Usha, B. Uma, Weakly nonlinear stability analysis of condensate/evaporating power-law liquid film down an inclined plane, ASME J. Appl. Mech. 70 (2003) 915–923.

[10] R. Usha, B. Uma, Interfacial phase change effects on the stability characteristics of thin viscoelastic liquid film down a vertical wall, Int. J. Eng. Sci. 42 (2004) 1381–1406.

[11] D.A. Edwards, H. Brenner, D.T. Wasan, Interfacial Transport Processes and Rheology, Butterworth-Heinemann, a Division of Reed Publishing Inc, USA, 1991.

[12] T.B. Benjamin, Wave formation in laminar flow down an inclined plane, J. Fluid Mech. 2 (1957) 554–574.

[13] C.S. Yih, Stability of liquid flow down an inclined plane, Phys. Fluids 6 (1963) 321–334.
[14] J.S. Tsai, C.I. Hung, C.K. Chen, Nonlinear hydromagnetic stability analysis of condensation film flow down a vertical plate, Acta Mechanica 118 (1996) 197–212.
[15] C.I. Hung, J.S. Tsai, C.K. Chen, Nonlinear Stability of the thin micropolar liquid film flowing down on a vertical plate, ASME J. Fluids Eng. 118 (1996) 498–505.
[16] S.W. Joo, S.H. Davis, S.G. Bankoff, Long-wave instabilities of heated falling films: two-dimensional theory of uniform layers, J. Fluid Mech. 230 (1991) 117–146.
[17] J.P. Burelbach, S.G. Bankoff, S.H. Davis, Nonlinear stability of evaporating/condensing liquid films, J. Fluid Mech. 195 (1988) 463–494.
[18] M.V.G. Krishna, S.P. Lin, Nonlinear stability of a viscous film with respect to three-dimensional side-band disturbance, Phys. Fluids 20 (1977) 1039–1044.
[19] V.L. Ginzburg, L.D. Landau, Theory of superconductivity, J. Exptl. Theoret. Phys. (USSR) 20 (1950) 1064–1082.
[20] W. Eckhaus, Studies in Nonlinear Stability, Springer, Berlin, 1965.
[21] J.S. Lin, C.I. Weng, Linear stability analysis of condensate film flow down a vertical cylinder, Chem. Eng. Comm. 57 (1987) 1–12.